Chapter IV

Extension to materially non linear problems

Content

Summary

In this chapter, the natural neighbours method (NEM) based on the FRAEIJS de VEUBEKE (FdV) variational principle is extended to materially non linear solids in 2D.

Considering a solid of unit thickness in plane strain state, the material has a non linear constitutive equation but the displacements of the solid are assumed to be very small.

Hence, the problem considered in this chapter is geometrically linear and materially non linear.

The FdV variational principle for linear elasticity (chapter II) is extended to the elasto-plastic case in which the assumed velocity, stresses, strain rates and surface support reactions are discretized separately.

The domain is decomposed into *N* Voronoi cells corresponding to the *N* nodes distributed inside the domain and on its boundary. Since the displacements are assumed to be infinitesimal, there is no need to update this decomposition as the solid deforms.

The following discretization hypotheses are admitted:

1. The assumed velocities are interpolated between the nodes with the Laplace interpolation function
2. The assumed strain rates are constant over each Voronoi cell *I*
3. The assumed stresses are constant over each Voronoi cell *I*
4. The assumed support reactions are constant over each edge *K* of Voronoi cells on which displacements are imposed.

Introducing these hypotheses in the extension of the FdV variational principle produces the set of equations governing the discretized solid.

The advantages of this method applied in linear elasticity remain valid in the extension to the elasto-plasticity problems:

- The equations do not require the calculation of the derivatives of the Laplace interpolation functions.
- In the absence of body forces, the equations only involve numerical integrations on the edges of the Voronoi cells.

It is possible to impose displacements $\widetilde{u}_i$ on any edge of any Voronoi cell in a weighted average sense.

Recasting the equations in matrix form, it is shown that the discretization parameters associated with the assumptions on the stresses and on the strain rates can be eliminated at the Voronoi cell level so that the final system of equations only involves the nodal velocities and the assumed support reactions.

If the displacements are only imposed as constant, the support reactions can be further eliminated from the final equation system.

This equation system can be solved step by step by integration on time and Newton-Raphson iterations at the level of the different time steps.

Using the von Mises elasto-plastic model with linear hardening, some applications are presented to evaluate the method.

Some patch tests are performed and show that this approach can pass the patch test successfully.

The method is then applied to the pure bending of a beam to study the convergence. The numerical solution is also compared to the results of another method based on the direct integration of the corresponding differential equations.

A square membrane with a hole is also used for convergence evaluation and for comparison with the finite element solution.

IV.1. Introduction

We consider a solid of unit thickness in plane strain state. The main notations are summarized in figure IV.1.

The material has non linear constitutive equation but the displacements of the solid are assumed to be very small.

Hence, the problem considered here is geometrically linear and materially non linear.

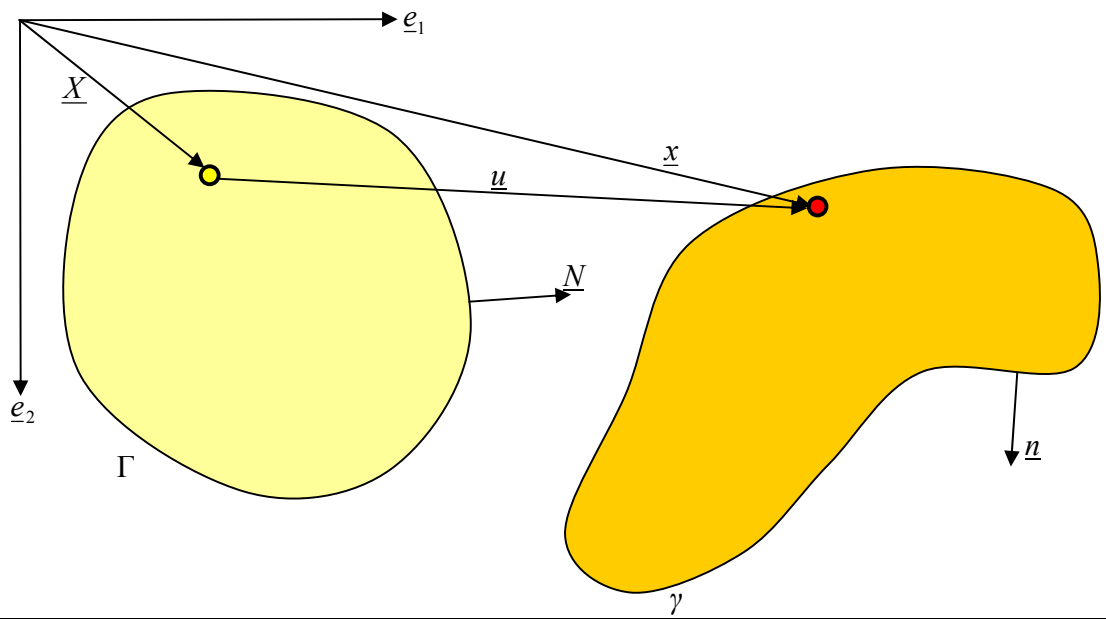

Notations	Initial configuration Γ	Deformed configuration γ
Area of the domain	A	a
Contour of the domain	S	s
Outside normal to the contour	$\underline{N}$	$\underline{n}$
Coordinates of material points	$\underline{X}$	$\underline{x}$
Body force (per unit volume)	$\underline{F}$	$\underline{f}$
Surface traction (per unit area)	$\underline{T}$	$\underline{t}$

Figure IV.1. Conventions for the non linear theory

In chapter II, section II.2, the classical approach of the natural neighbours method (NEM) has been introduced and developed in chapter III for linear elastic problems.

In this chapter, we will start from a rate form of the FRAEIJS de VEUBEKE (FdV) variational principle (chapter II, section II.3) to develop an extension of the NEM to materially non linear problems, i.e. problems in which the displacements remain very small but the material constitutive equation is non linear, for example elasto-platic or elasto-visco-plastic.

Hence, referring to figure IV.1, the initial configuration Γ and the deformed configuration γ are very close to each other.

The domain is decomposed into N Voronoi cells corresponding to N nodes distributed inside the domain and on its boundary.

Since the problem is geometrically linear, the domain decomposition remains valid through the deformation process.

After discretization of the velocity field, the stress field, the strain rate field and the support reactions field, we get an equation system that can be solved with the help of Newton-Raphson iterations at each time step.

As an example of non linear constitutive equation, the elasto-plastic von Mises linear hardening model is used to perform some applications to evaluate the method.

In the NEM for linear elastic problems (chapter III), we have seen that:

- the derivatives of the Laplace interpolation functions are not necessary,
- only numerical integration on the edges of the Voronoi cells are required,
- incompressibility locking is avoided.

In this chapter, we will see that these properties remain valid for non linear problems.

IV.2. Non linear theory

The following variational equations constitute the starting point of the approach. They are an extension of the variational approach proposed by FRAEIJS de VEUBEKE for linear elasticity.

$$\delta\Pi_1 = \int_a \sigma_{ij}\, \delta\dot{\varepsilon}_{ij}\, da \tag{IV.1}$$

$$\delta\Pi_2 = \int_a \Sigma_{ij} \left[\frac{1}{2}\left(\frac{\partial \delta\dot{u}_i}{\partial x_j} + \frac{\partial \delta\dot{u}_j}{\partial x_i}\right) - \delta\dot{\varepsilon}_{ij} \right] da \tag{IV.2}$$

$$\delta\Pi_3 = \int_a \delta\Sigma_{ij} \left[\frac{1}{2}\left(\frac{\partial \dot{u}_i}{\partial x_j} + \frac{\partial \dot{u}_i}{\partial x_j}\right) - \dot{\varepsilon}_{ij} \right] da \tag{IV.3}$$

$$\delta\Pi_4 = -\int_a f_i\,\delta\dot{u}_i\,da \tag{IV.4}$$

$$\delta\Pi_5 = -\oint_{s_t} t_i\,\delta\dot{u}_i\,ds \tag{IV.5}$$

$$\delta\Pi_6 = \int_{s_u} \delta r_i(\dot{\tilde{u}}_i - \dot{u}_i)\,ds - \int_{s_u} r_i\,\delta\dot{u}_i\,ds \tag{IV.6}$$

$$\delta\Pi(\dot{u}_i, \dot{\varepsilon}_{ij}, \Sigma_{ij}, r_i) = \delta\Pi_1 + \delta\Pi_2 + \delta\Pi_3 + \delta\Pi_4 + \delta\Pi_5 + \delta\Pi_6 = 0 \tag{IV.7}$$

with

$\dot{u}_i$ the assumed velocity field,

$\dot{\varepsilon}_{ij}$ the assumed strain rate field,

Σ_{ij} the assumed stress field,

r_i the assumed support reaction field.

In (IV.1), σ_{ij} are the constitutive stresses at the considered material point in the deformed configuration.

For inelastic materials, these stresses are usually obtained by integration, along the strain path of the considered material point, of a system of equations of the type:

$$\overset{\nabla}{\sigma}_{ij} = f_{ij}(\sigma_{ij}, q_{ij}, \dot{\varepsilon}_{ij}) \tag{IV.8}$$

$$\overset{\nabla}{q}_{ij} = h_{ij}(\sigma_{ij}, q_{ij}) \tag{IV.9}$$

with q_{ij} a set of internal variables and where the superscript $\overset{\nabla}{}$ is the symbol for an objective derivative (in the particular case of a geometrically linear problem, a simple time derivative is sufficient) .

In (IV.5) and (IV.6), some integrals are computed along the domain contour. This contour is the union of some of the edges of some Voronoi cells. These edges are denoted by s_K and we have

$$s = \sum_{K=1}^{M} s_K\ ; \qquad s_u = \sum_{K=1}^{M_u} s_K\ ; \qquad s_t = \sum_{K=1}^{M_t} s_K\ ; \qquad s = s_u \cup s_t \Rightarrow M = M_u + M_t$$

where M is the number of edges composing the contour, M_u the number of edges on which displacements $\tilde{u}_i$ are imposed and M_t the number of edges on which surface tractions t_i are imposed.

The Euler equations corresponding to the variational equation (IV.7) are summarized in table IV.1.

Table IV.1. Euler equations deduced from the Fraeijs de Veubeke variational principle		
Variation	Equation	Comments
$\delta\dot{\varepsilon}_{ij}$ in a	$\sigma_{ij} = \Sigma_{ij}$	The assumed stresses are identified as the constitutive stresses inside the domain
$\delta\Sigma_{ij}$ in a	$\dot{\varepsilon}_{ij} = \frac{1}{2}(\frac{\partial \dot{u}_i}{\partial x_j} + \frac{\partial \dot{u}_j}{\partial x_i})$	Compatibility between the assumed strain rates and the assumed velocities inside the domain
δr_i on s_u	$\dot{u}_i = \dot{\tilde{u}}_i$	Compatibility between the assumed velocities and the velocities imposed on the part s_u of the domain contour
$\delta\dot{u}_i$ in a	$\frac{\partial \Sigma_{ji}}{\partial x_j} + f_i = 0$	Equilibrium inside the domain between the assumed stresses and the body forces
$\delta\dot{u}_i$ on s_t	$n_j \Sigma_{ji} = t_i$	Equilibrium on the part s_t of the domain contour where surface tractions are imposed

IV.3. Domain decomposition

The domain contains N nodes (including nodes on the domain contour) and is decomposed into N Voronoi cells, each cell corresponding to a node.

Since the problem is geometrically linear, the domain decomposition remains valid throughout the deformation process.

The area of the domain is:

$$a = \sum_{I=1}^{N} a_I \tag{IV.10}$$

with a_I the area of cell I.

We denote c_I the contour of Voronoi cell n° I.

Then

$$\delta\Pi_1 = \sum_{I=1}^{N} \int_{a_I} \sigma_{ij}\, \delta\dot{\varepsilon}_{ij}\, da_I \tag{IV.11}$$

$$\delta\Pi_2 = \sum_{I=1}^{N} \int_{a_I} \Sigma_{ij} \left[\frac{1}{2}(\frac{\partial \delta\dot{u}_i}{\partial x_j} + \frac{\partial \delta\dot{u}_j}{\partial x_i}) - \delta\dot{\varepsilon}_{ij} \right] da_I \tag{IV.12}$$

$$\delta\Pi_3 = \sum_{I=1}^{N} \int_{a_I} \delta\Sigma_{ij} \left[\frac{1}{2}(\frac{\partial \dot{u}_i}{\partial x_j} + \frac{\partial \dot{u}_j}{\partial x_i}) - \dot{\varepsilon}_{ij} \right] da_I \tag{IV.13}$$

$$\delta\Pi_4 = -\sum_{I=1}^{N} \int_{a_I} f_i \, \delta\dot{u}_i \, da_I \tag{IV.14}$$

$$\delta\Pi_5 = -\sum_{K=1}^{M_t} \int_{s_K} t_i \, \delta\dot{u}_i \, ds_K \tag{IV.15}$$

$$\delta\Pi_6 = \sum_{K=1}^{M_u} \left[\int_{s_K} \delta r_i (\tilde{\dot{u}}_i - \dot{u}_i) \, ds_K - \int_{s_K} r_i \, \delta\dot{u}_i \, ds_K \right] \tag{IV.16}$$

IV.4. Discretization

We make the following discretization hypotheses:

1. The assumed strain rates $\dot{\varepsilon}_{ij}$ are constant over each Voronoi cell *I*:

$$\dot{\varepsilon}_{ij} = \dot{\varepsilon}_{ij}^{I} \tag{IV.17}$$

2. The assumed stresses Σ_{ij} are constant over each Voronoi cell *I*:

$$\Sigma_{ij} = \Sigma_{ij}^{I} \tag{IV.18}$$

3. The assumed support reactions r_i are constant over each edge *K* of Voronoi cells on which displacements are imposed

$$r_i = r_i^K \tag{IV.19}$$

4. The assumed velocities $\dot{u}_i$ are interpolated by Laplace interpolation functions:

$$\dot{u}_i = \sum_{J=1}^{N} \Phi_J \, \dot{u}_i^J \tag{IV.20}$$

where $\dot{u}_i^J$ is the velocity of node *J* (corresponding to the Voronoi cell *J*).

As a consequence of (IV.8, IV.9 and IV.17), the stresses σ_{ij} are constant over each Voronoi cell *I*:

$$\sigma_{ij} = \sigma_{ij}^{I} \tag{IV.21}$$

The variations of the independent variables are:

$$\delta\dot{\varepsilon}_{ij} = \delta\dot{\varepsilon}_{ij}^{I} \tag{IV.22}$$

$$\delta\Sigma_{ij} = \delta\Sigma_{ij}^{I} \tag{IV.23}$$

$$\delta r_i = \delta r_i^K \tag{IV.24}$$

$$\delta\dot{u}_i = \sum_{I=1}^{N} \Phi_I \, \delta\dot{u}_i^I \tag{IV.25}$$

Introducing these assumptions in (IV.11) to (IV.16), and integrating by parts, we get:

$$\delta\Pi_1 = \sum_{I=1}^{N} \sigma_{ij}^I \, \delta\dot{\varepsilon}_{ij}^I \, a_I \tag{IV.26}$$

$$\delta\Pi_2 = \sum_{I=1}^{N} \Sigma_{ij}^I \int_{A_I} \left[\frac{1}{2} \left(\frac{\partial \delta\dot{u}_i}{\partial X_j} + \frac{\partial \delta\dot{u}_j}{\partial X_i} \right) \right] da_I - \sum_{I=1}^{N} \Sigma_{ij}^I \, \delta\dot{\varepsilon}_{ij}^I \, a_I =$$

$$\sum_{I=1}^{N} \Sigma_{ij}^I \oint_{c_I} n_j^I \delta\dot{u}_i \, dc_I - \sum_{I=1}^{N} \Sigma_{ij}^I \, \delta\dot{\varepsilon}_{ij}^I \, a_I \tag{IV.27}$$

$$\delta\Pi_3 = \sum_{I=1}^{N} \delta\Sigma_{ij}^I \int_{A_I} \left[\frac{1}{2} \left(\frac{\partial \dot{u}_i}{\partial X_j} + \frac{\partial \dot{u}_j}{\partial X_i} \right) \right] da_I - \sum_{I=1}^{N} \delta\Sigma_{ij}^I \, \dot{\varepsilon}_{ij}^I \, a_I =$$

$$\sum_{I=1}^{N} \delta\Sigma_{ij}^I \oint_{c_I} n_j^I \dot{u}_i \, dc_I - \sum_{I=1}^{N} \delta\Sigma_{ij}^I \, \dot{\varepsilon}_{ij}^I \, a_I \tag{IV.28}$$

$$\delta\Pi_6 = \sum_{K=1}^{M_u} \left[\delta r_i^K \int_{s_K} (\dot{\tilde{u}}_i - \dot{u}_i) \, ds_K - r_i^K \int_{s_K} \delta\dot{u}_i \, ds_K \right] \tag{IV.29}$$

where n_j^I is the outward normal to the contour of Voronoi cell *I*.

Introducing in (IV.7), we get:

$$\delta\Pi = \delta\Pi_{VA} + \delta\Pi_{VC} + \delta\Pi_{DC} + \delta\Pi_{EF} = 0 \tag{IV.30}$$

with

$$\delta\Pi_{VA} = \sum_{I=1}^{N} (\sigma_{ij}^I - \Sigma_{ij}^I) \delta\dot{\varepsilon}_{ij}^I \, a_I - \sum_{I=1}^{N} \delta\Sigma_{ij}^I \, \dot{\varepsilon}_{ij}^I \, a_I \tag{IV.31}$$

$$\delta\Pi_{VC} = \sum_{I=1}^{N} \Sigma_{ij}^I \oint_{c_I} n_j^I \, \delta\dot{u}_i \, dc_I + \sum_{I=1}^{N} \delta\Sigma_{ij}^I \oint_{c_I} n_j^I \, \dot{u}_i \, dc_I \tag{IV.32}$$

$$\delta\Pi_{DC} = \sum_{K=1}^{M_u} \left[\delta r_i^K \int_{s_K} (\dot{\tilde{u}}_i - \dot{u}_i) \, ds_K - r_i^K \int_{s_K} \delta\dot{u}_i \, ds_K \right] \tag{IV.33}$$

$$\delta\Pi_{EF} = -\sum_{I=1}^{N} \int_{a_I} f_i \, \delta\dot{u}_i \, da_I - \sum_{K=1}^{M_t} \int_{s_K} t_i^K \, \delta\dot{u}_i \, ds_K \tag{IV.34}$$

In (IV.32) to (IV.34), the velocities and virtual velocities are interpolated by (IV.20) and (IV.25) respectively. Substituting in (IV.32), we get:

$$\delta\Pi_{VC} = \sum_{I=1}^{N} \Sigma_{ij}^{I} \left[\sum_{J=1}^{N} \oint_{c_I} n_j^I \Phi_J \delta\dot{u}_i^J \, dc_I \right] + \sum_{I=1}^{N} \delta\Sigma_{ij}^{I} \left[\sum_{J=1}^{N} \oint_{c_I} n_j^I \Phi_J \dot{u}_i^J \, dc_I \right] \tag{IV.35}$$

Finally, since the edges of the Voronoi cell are straight lines, the outside normal n_j to edge s_K is constant along this edge and is denoted n_j^K

Now, using the discretization (IV.20), we get:

$$\delta\Pi_{DC} = \sum_{K=1}^{M_u} \delta r_i^K \left\{ \int_{s_K} \dot{\tilde{u}}_i ds_K - \sum_{J=1}^{N} \dot{u}_i^J \int_{s_K} \Phi_J ds_K \right\} - \sum_{K=1}^{M_u} r_i^K \left\{ \sum_{J=1}^{N} \delta\dot{u}_i^J \int_{s_K} \Phi_J ds_K \right\} \tag{IV.36}$$

Similarly, (IV.34) becomes:

$$\delta\Pi_{EF} = -\sum_{I=1}^{N} \sum_{J=1}^{N} \delta\dot{u}_i^J \int_{a_I} f_i \Phi_J \, da_I - \sum_{K=1}^{M_t} \sum_{J=1}^{N} \delta u_i'^J \int_{s_K} t_i \Phi_J \, ds_K \tag{IV.37}$$

Collecting all the results, we obtain the discretized rate form of the FdV variational principle.

$$\begin{aligned}
\delta\Pi = & \sum_{I=1}^{N} (\sigma_{ij}^I - \Sigma_{ij}^I) \delta\dot{\varepsilon}_{ij}^I \, a_I - \sum_{I=1}^{N} \delta\Sigma_{ij}^I \dot{\varepsilon}_{ij}^I \, a_I \\
& + \sum_{I=1}^{N} \Sigma_{ij}^I \left\{ \sum_{J=1}^{N} \delta\dot{u}_i^J \oint_{c_I} n_j^I \Phi_J dc_I \right\} \\
& + \sum_{I=1}^{N} \delta\Sigma_{ij}^I \left\{ \sum_{J=1}^{N} \dot{u}_i^J \oint_{c_I} n_j^I \Phi_J dc_I \right\} \\
& + \sum_{K=1}^{M_u} \delta r_i^K \left\{ \int_{s_K} \dot{\tilde{u}}_i ds_K - \sum_{J=1}^{N} \dot{u}_i^J \int_{s_K} \Phi_J ds_K \right\} \\
& - \sum_{K=1}^{M_u} r_i^K \left\{ \sum_{J=1}^{N} \delta\dot{u}_i^J \int_{s_K} \Phi_J ds_K \right\} \\
& - \sum_{I=1}^{N} \sum_{J=1}^{N} \delta\dot{u}_i^J \int_{a_I} f_i \Phi_J \, da_I - \sum_{K=1}^{M_t} \sum_{J=1}^{N} \delta\dot{u}_i^J \int_{s_K} t_i \Phi_J ds_K \quad = 0
\end{aligned} \tag{IV.38}$$

IV.5. Equations deduced from the FdV variational principle

Let us reorganize the terms of (IV.38)

$$\delta\Pi = \sum_{I=1}^{N} \delta\dot{\varepsilon}_{ij}^{I} \left\{ (\sigma_{ij}^{I} - \Sigma_{ij}^{I})\, a_I \right\}$$
$$+ \sum_{I=1}^{N} \delta\Sigma_{ij}^{I} \left\{ -\dot{\varepsilon}_{ij}^{I}\, a_I + \sum_{J=1}^{N} \dot{u}_i^J\, A_j^{IJ} \right\}$$
$$+ \sum_{K=1}^{M_u} \delta r_i^K \left\{ \dot{\tilde{U}}_i^K - \sum_{J=1}^{N} \dot{u}_i^J\, B^{KJ} \right\}$$
$$+ \sum_{J=1}^{N} \delta\dot{u}_i^J \left\{ \sum_{I=1}^{N} (\Sigma_{ij}^{I} A_j^{IJ} - \tilde{f}_i^{IJ}) - \sum_{K=1}^{M_u} r_i^K B^{KJ} - \sum_{K=1}^{M_t} \tilde{t}_i^{KJ} \right\} = 0 \qquad \text{(IV.39)}$$

In this result, the following notations have been used.

$$A_j^{IJ} = \oint_{c_I} n_j^I \Phi_J\, dc_I \qquad \text{(IV.40)}$$

$$B^{KJ} = \int_{s_K} \Phi_J\, ds_K \qquad \text{(IV.41)}$$

$$\dot{\tilde{U}}_i^K = \int_{s_K} \dot{\tilde{u}}_i\, ds_K \qquad \text{(IV.42)}$$

$$\tilde{f}_i^{IJ} = \int_{a_I} f_i \Phi_J\, da_I \qquad \text{(IV.43)}$$

$$\tilde{t}_i^{KJ} = \int_{s_K} t_i \Phi_J\, ds_K \qquad \text{(IV.44)}$$

Equation (IV.40) involves the integration on the contour c_I of Voronoi cell *I*.

Equations (IV.41) and (IV.42) involve the integration on the edge s_K (belonging to the domain contour) of a Voronoi cell.

We are now able to deduce the discretized Euler equations.

1. In all the Voronoi cells *I*

   $$\sigma_{ij}^{I} = \Sigma_{ij}^{I} \qquad \text{for} \quad I = 1, N \qquad \text{(IV.45)}$$

   These equations identify the assumed stresses Σ_{ij}^{I} as the constitutive stresses σ_{ij}^{I} deduced from the constitutive equations (IV.8) and (IV.9) and from the assumed strains rates $\dot{\varepsilon}_{ij}^{I}$ in each Voronoi cell.

2. In all the Voronoi cells *I*

$$\dot{\varepsilon}_{ij}^{I}\, a_I = \sum_{J=1}^{N} \dot{u}_i^J\, a_j^{IJ} \tag{IV.46}$$

This is a compatibility equation linking the assumed strain rate $\dot{\varepsilon}_{ij}^{I}$ in Voronoi cell I with the assumed nodal velocity $\dot{u}_i^J$.

3. On the edges $K = 1, M_u$ of Voronoi cells submitted to imposed velocities

$$\sum_{J=1}^{N} \dot{u}_i^J B^{KJ} = \dot{\tilde{U}}_i^K \tag{IV.47}$$

These are also compatibility equations taking account of the imposed velocities $\dot{\tilde{u}}_i$ on the part s_u of the domain contour.

4. In all the Voronoi cells J

$$\sum_{I=1}^{N} (\Sigma_{ij}^{I} A_j^{IJ} - \tilde{f}_i^{IJ}) - \sum_{K=1}^{M_t} \tilde{t}_i^{KJ} - \sum_{K=1}^{M_u} r_i^K B^{KJ} = 0 \tag{IV.48}$$

These are equilibrium equations taking account of the body forces f_i, the surface tractions t_i and the support reactions r_i.

We note that, in the developments above, the only term that implies an integration over the area of the Voronoi cells is $\tilde{f}_i^{IJ} = \int_{a_I} f_i \Phi_J \, da_I$.

Hence, if there are no body forces, the problem of choosing integration points is simplified: there are only integrations along the straight edges of Voronoi cells. A classical Gauss integration scheme can be used. In chapter III, some tests have shown that 2 integration points give enough precision.

Furthermore, this formulation does not require the derivatives of the shape functions.

In the linear elastic problem (Chapter III), using the FdV functional as starting point, we obtained the same advantages as with the stabilized confofming integration [CHEN J. S. et al. (2001), YOO J. et al. (2004)]. This property remains valid in non linear problem.

Finally, in the approach developed here, it is possible to impose displacements $\tilde{u}_i$ on any edge of any Voronoi cell. From (IV.42) and (IV.47), it is clear that the imposed displacements are respected in a weighted average sense.

IV.6. Matrix notation

We introduce the following matrix notations.

$$\{\dot{u}\}^I = \begin{Bmatrix} \dot{u}_1^I \\ \dot{u}_2^I \end{Bmatrix}; \quad \{\tilde{f}\}^{IJ} = \begin{Bmatrix} \tilde{f}_1^{IJ} \\ \tilde{f}_2^{IJ} \end{Bmatrix}; \quad \{\tilde{t}\}^{KJ} = \begin{Bmatrix} \tilde{t}_1^{KJ} \\ \tilde{t}_2^{KJ} \end{Bmatrix}; \tag{IV.49}$$

$$\left\{\tilde{f}\right\}^J = \sum_{I=1}^{N} \left\{\tilde{f}\right\}^{IJ} \; ; \quad \left\{\tilde{t}\right\}^J = \sum_{K=1}^{M_t} \left\{\tilde{t}\right\}^{KJ} \tag{IV.50}$$

$$\left\{\dot{\varepsilon}\right\}^I = \begin{Bmatrix} \dot{\varepsilon}_{11}^I \\ \dot{\varepsilon}_{22}^I \\ 2\dot{\varepsilon}_{12}^I \end{Bmatrix}; \quad \left\{\sigma\right\}^I = \begin{Bmatrix} \sigma_{11}^I \\ \sigma_{22}^I \\ \sigma_{12}^I \end{Bmatrix}; \quad \left\{\Sigma\right\}^I = \begin{Bmatrix} \Sigma_{11}^I \\ \Sigma_{22}^I \\ \Sigma_{12}^I \end{Bmatrix} \tag{IV.51}$$

$$\left[A\right]^{IJ} = \begin{bmatrix} A_1^{IJ} & 0 & A_2^{IJ} \\ 0 & A_2^{IJ} & A_1^{IJ} \end{bmatrix}; \quad \left\{r\right\}^K = \begin{Bmatrix} r_1^K \\ r_2^K \end{Bmatrix}; \quad \left\{\dot{\tilde{U}}\right\}^K = \begin{Bmatrix} \dot{\tilde{U}}_2^K \\ \dot{\tilde{U}}_1^K \end{Bmatrix} \tag{IV.52}$$

Then, we get successively:

$$\sigma_{ij}^I = \Sigma_{ij}^I \Rightarrow \left\{\sigma\right\}^I = \left\{\Sigma\right\}^I \tag{IV.53}$$

$$\Sigma_{ij}^I A_j^{IJ} \Rightarrow \left[A\right]^{IJ} \left\{\Sigma\right\}^I \; ; \quad \tilde{f}^{IJ} \Rightarrow \left\{\tilde{f}\right\}^{IJ} ; \quad \tilde{t}^{IJ} \Rightarrow \left\{\tilde{t}\right\}^{IJ} \tag{IV.54}$$

$$\sum_{I=1}^{N} \Sigma_{ij}^I A_j^{IJ} - \sum_{K=1}^{M_u} r_i^K B^{KJ} = \sum_{I=1}^{N} \tilde{f}_i^{IJ} + \sum_{K=1}^{M_t} \tilde{t}_i^{KJ} \Rightarrow \sum_{I=1}^{N} \left[A\right]^{IJ} \left\{\Sigma\right\}^I - \sum_{K=1}^{M_u} B^{KJ} \left\{r\right\}^K = \left\{\tilde{f}\right\}^J + \left\{\tilde{t}\right\}^J \tag{IV.55}$$

The term $\sum_{I=1}^{N} \left[A\right]^{IJ} \left\{\Sigma\right\}^I - \sum_{K=1}^{M_u} B^{KJ} \left\{r\right\}^K$ is the interior nodal force at node *J*, i.e. in cell *J*.

It is the sum of the contributions $\left[A\right]^{IJ} \left\{\Sigma\right\}^I$ of the stresses Σ_{ij}^I existing in all the Voronoi cells *I* and of the contributions $B^{KJ} \left\{r\right\}^K$ of the support reactions r_i^K existing on the contour edges *K* where velocities are imposed.

The term $\left\{\tilde{f}\right\}^J + \left\{\tilde{t}\right\}^J$ is the exterior nodal force at node *J*, i.e. in cell *J*. It is the sum of :

- the contributions $\left\{\tilde{f}\right\}^{IJ}$ of the body forces F_i existing in all the Voronoi cells *I*
- the contributions $\left\{\tilde{t}\right\}^{IJ}$ of the surface tractions t_i applied on the part s_t of the domain contour.

Now, consider equation (IV.46). It can be written

$$a_I \left\{\dot{\varepsilon}\right\}^I = \sum_{J=1}^{N} \left[A\right]^{IJ,T} \left\{\dot{u}\right\}^J \tag{IV.56}$$

where $\left[A\right]^{IJ,T}$ is the transpose of $\left[A\right]^{IJ}$.

Note that in $\left\{\dot{\varepsilon}\right\}^I$, the third component is $2\dot{\varepsilon}_{12}^I$.

The compatibility equation (IV.56) defines the strain rate $\{\dot{\varepsilon}\}^I$ in a Voronoi cell I as the sum of the contributions $[A]^{IJ,T}\{\dot{u}\}^J$ of all the nodes J.

On the edges K submitted to imposed velocities, we must consider (IV.47) that becomes

$$\sum_{J=1}^{N} B^{KJ}\{\dot{u}\}^J = \{\tilde{\dot{U}}\}^K \qquad \text{(IV.57)}$$

The tables IV.2 and IV.3 below collect all the results in matrix form.

In these tables, taking account of (IV.53), $\{\Sigma\}^I$ is replaced by $\{\sigma\}^I$

Table IV.2 Matrix notations for the materially non linear case.

Notations and symbols	Comments
$\{\dot{\varepsilon}\}^I = \begin{Bmatrix} \dot{\varepsilon}_{11}^I \\ \dot{\varepsilon}_{22}^I \\ 2\dot{\varepsilon}_{12}^I \end{Bmatrix}$	Strains in cell I
$\{\sigma\}^I = \begin{Bmatrix} \sigma_{11}^I \\ \sigma_{22}^I \\ \sigma_{12}^I \end{Bmatrix}$	Stresses in cell I
$\{\dot{u}\}^I = \begin{Bmatrix} \dot{u}_1^I \\ \dot{u}_2^I \end{Bmatrix}$	Displacements velocity of node I belonging to cell I
$\{r\}^K = \begin{Bmatrix} r_1^K \\ r_2^K \end{Bmatrix}$	Support reactions on edge K submitted to imposed displacements
a_I ; c_I	Area and contour of cell I
s_K	Length of edge K of a cell
Φ_J	Interpolant associated with node J
$\tilde{f}_i^{IJ} = \int_{a_I} f_i \Phi_J \, da_I$; $\{\tilde{f}\}^{IJ} = \begin{Bmatrix} \tilde{f}_1^{IJ} \\ \tilde{f}_2^{IJ} \end{Bmatrix}$; $\{\tilde{f}\}^J = \sum_{I=1}^{N} \{\tilde{f}\}^{IJ}$	$\{\tilde{f}\}^J$ is the nodal force at node J equivalent to the body forces f_i applied to the solid

$\tilde{t}_i^{KJ} = \int_{s_K} t_i \Phi_J \, ds_K \; ; \; \{\tilde{t}\}^{KJ} = \begin{Bmatrix} \tilde{t}_1^{KJ} \\ \tilde{t}_2^{KJ} \end{Bmatrix} ;$ $\{\tilde{t}\}^J = \sum_{K=1}^{M_t} \{\tilde{t}\}^{KJ}$	$\{\tilde{t}\}^J$ is the nodal force at node J equivalent to the surface tractions t_i applied to the contour of the solid
$\dot{\tilde{U}}_i^K = \int_{s_K} \dot{\tilde{u}}_i ds_K \; ; \; \{\dot{\tilde{U}}\}^K = \begin{Bmatrix} \dot{\tilde{U}}_2^K \\ \dot{\tilde{U}}_1^K \end{Bmatrix}$	$\{\dot{\tilde{U}}\}^K$ is a generalized displacement velocity taking account of imposed velocities $\dot{\tilde{u}}_i$ on edge K
$B^{KJ} = \int_{s_K} \Phi_J ds_K$	Integration over the edge K of a cell
$A_j^{IJ} = \oint_{c_I} n_j^I \Phi_J \, dc_I \; ; \; [A]^{IJ} = \begin{bmatrix} A_1^{IJ} & 0 & A_2^{IJ} \\ 0 & A_2^{IJ} & A_1^{IJ} \end{bmatrix}$	A_j^{IJ} can also be computed by $A_j^{IJ} = \sum_{all\ K(I)} n_j^{K(I)} B^{K(I)J}$

Table IV.3. Discretized equations in matrix form for the materially non linear case

Equations	Comments	
$\sum_{I=1}^{N} [A]^{IJ} \{\sigma\}^I - \sum_{K=1}^{M_u} B^{KJ} \{r\}^K = \{\tilde{f}\}^J + \{\tilde{t}\}^J$	Equilibrium equation of cell J	(IV.58)
$a_I \begin{Bmatrix} \& \\ \varepsilon \end{Bmatrix}^I = \sum_{J=1}^{N} [A]^{IJ,T} \begin{Bmatrix} \& \\ u \end{Bmatrix}^J$	Compatibility equation for cells I	(IV.59)
$\sum_{J=1}^{N} B^{KJ} \{\dot{u}\}^J = \{\dot{\tilde{U}}\}^K$	Compatibility equation on edge K submitted to imposed velocities	(IV.60)

IV.7. Solution of the equations

The equations to solve are:

- The equilibrium equations for all the Voronoi cells J

$$\sum_{I=1}^{N} [A]^{IJ} \{\Sigma\}^I - \sum_{K=1}^{M_u} B^{KJ} \{r\}^K = \{\tilde{f}\}^J + \{\tilde{t}\} \qquad \text{(IV.61)}$$

- The compatibility equations in all the Voronoi cells I

$$a_I \{\dot{\varepsilon}\}^I = \sum_{J=1}^{N} [A]^{IJ,T} \{\dot{u}\}^J \qquad \text{(IV.62)}$$

- The compatibility equation on edge *K* submitted to imposed velocities

$$\sum_{J=1}^{N} B^{KJ} \{\dot{u}\}^J = \{\dot{\tilde{U}}\}^K \qquad \text{(IV.63)}$$

Integrating (IV.63) in time, we get

$$\sum_{J=1}^{N} B^{KJ} \{u(t)\}^J = \{\tilde{U}(t)\}^K \qquad \text{(IV.64)}$$

With the notations

$$\{q\} = \begin{Bmatrix} \{u\}^1 \\ \{u\}^2 \\ . \\ . \\ \{u\}^N \end{Bmatrix}; \quad \{\tilde{f}\} = \begin{Bmatrix} \{\tilde{f}\}^1 \\ \{\tilde{f}\}^2 \\ . \\ . \\ \{\tilde{f}\}^N \end{Bmatrix}; \quad \{\tilde{t}\} = \begin{Bmatrix} \{\tilde{t}\}^1 \\ \{\tilde{t}\}^2 \\ . \\ . \\ \{\tilde{t}\}^N \end{Bmatrix}; \quad \{\tilde{Q}\} = \{\tilde{F}\} + \{\tilde{T}\}$$

equation (IV.64), in matrix form, becomes $[B]^T \{q(t)\} = \{\tilde{U}(t)\}$ where $\{\tilde{U}(t)\}$ is a column matrix containing generalized displacements imposed to some nodes at time *t*.

This constitutes a set of constraints on the nodal displacements $\{q(t)\}$ deserving the same remarks as in the linear elastic case.

In particular, if displacements $\tilde{u}_i = 0$ are imposed at any time *t* on the segment *CD* joining 2 nodes *C* and *D* of the domain contour, it is easy to show that (IV.64) leads to $u_i^C(t) = 0$ and $u_i^D(t) = 0$ at any time *t*.

In such a case, the displacements u_i^C and u_i^D can be removed from the unknowns $\{q\}$.

This reasoning can be extended to the case of displacements imposed to zero on any number of similar segments belonging to the contour.

For the solution of the equations, a classical step by step procedure is used.

Assume that (IV.61) and (IV.62) are satisfied at time t_A so that we know exactly the values of:

$${}^A\sigma_{ij}^J,\ {}^A\dot{\varepsilon}_{ij}^J,\ {}^A\dot{u}_i^J,\ {}^Au_i^J,\ {}^A\tilde{f}_i^J,\ {}^A\tilde{t}_i^J,\ {}^A\tilde{u}_i^J,\ {}^Ar_i^J$$

We want to calculate, at time $t_B = t_A + \Delta t$,

$${}^B\sigma_{ij}^J,\ {}^B\dot{\varepsilon}_{ij}^J,\ {}^B\dot{u}_i^J,\ {}^Br_i^J$$

and at time t_B, (IV.61) and (IV.62) must be satisfied.

Let $${}^B\sigma_{ij}^J = {}^A\sigma_{ij}^J + \Delta\sigma_{ij}^J \qquad \text{(IV.65)}$$

$$ {}^{B}u_i^J = {}^{A}u_i^J + \Delta u_i^J \tag{IV.66} $$

During the time interval Δt, we assume the evolution of the displacements is a linear function of time:

$$ \dot{u}_i^J = \frac{{}^{B}u_i^J - {}^{A}u_i^J}{\Delta t} = \frac{\Delta u_i^J}{\Delta t} \tag{IV.67} $$

If ${}^{B}u_i^J$ is known, we can calculate $\dot{u}_i^J$ by (IV.67) and $\dot{\varepsilon}_{ij}^J$ by (IV.62).

Then we can calculate the stresses ${}^{B}\sigma_{ij}^J$ in each Voronoi cell by integration of the constitutive equation.

What we have to do is to find the value of ${}^{B}u_i^J$ such that (IV.61) can be satisfied.

We proceed by iterations.

Let $\left(\Delta u_i^J\right)_k$ be the value of Δu_i^J at iteration k and $\left(\Delta u_i^J\right)_{k+1}$ be the value of Δu_i^J at iteration $k+1$.

Let $\left(\Delta u_i^J\right)_{k+1} = \left(\Delta u_i^J\right)_k + du_i^J$ (IV.68)

After some developments, we get:

$$ \sum_{I=1}^{N}\left[\left({}^{B}\sigma_{ij}^I\right)_k A_j^{IJ}\right] - {}^{B}\widetilde{t}_i^J - {}^{B}\widetilde{f}_i^J - \left(p_i^J\right)_k = \left(R_i^J\right)_k \neq 0 \tag{IV.69} $$

$$ \sum_{I=1}^{N}\left[\left({}^{B}\sigma_{ij}^I\right)_{k+1} A_j^{IJ}\right] - {}^{B}\widetilde{t}_i^J - {}^{B}\widetilde{f}_i^J - \left(p_i^J\right)_{k+1} = 0 \tag{IV.70} $$

where $\{p\}^J = \sum_{K=1}^{M_u} B^{KJ}\{r\}^K$ (IV.71)

and $(R_i^J)_k$ is the out of balance force at node J for iteration k.

From (IV.69), (IV.70), we get:

$$ \sum_{I=1}^{N} d\sigma_{ij}^I A_j^{IJ} + \left(R_i^J\right)_k + \left(p_i^J\right)_k - \left(p_i^J\right)_{k+1} = 0 \tag{IV.72} $$

This equation gives the $d\sigma_{ij}^I$ that we should have in order to ensure equilibrium at the end of the iteration.

From the constitutive equations of the material and according to the integration scheme used to integrate them, we can write:

$$\begin{Bmatrix} d\sigma_{11} \\ d\sigma_{22} \\ d\sigma_{12} \end{Bmatrix}^I = \left[C_t^I\right] \begin{Bmatrix} \dot{\varepsilon}_{11} \\ \dot{\varepsilon}_{22} \\ \dot{\varepsilon}_{12} \end{Bmatrix}^I \Delta t \qquad \text{(IV.73)}$$

where $\left[C_t^I\right]$ is the consistent compliance matrix which has to be calculated for each constitutive equation.

Finally, from (IV.62) :

$$d\dot{\varepsilon}_{ij}^I a_I = \sum_{J=1}^{N} \frac{du_i^J A_j^{IJ}}{\Delta t} \qquad \text{(IV.74)}$$

Equation (IV.74) provides the link between the du_i^J that we want to compute and the $d\dot{\varepsilon}_{ij}^I$.

From (IV.72), (IV.73) and (IV.74), we get the following equation system:

$$\left[M\right]\{dq\} = \{dQ\} \qquad \text{(IV.75)}$$

with

$$\left[M\right]^{JL} = \sum_{I=1}^{N} [A]^{IJ} \left[\mathrm{C}^*\right]^I [A]^{IL} \qquad \text{(IV.76)}$$

$$\left[M\right] = \begin{bmatrix} [M]^{11} & [M]^{12} & . & . & [M]^{1N} \\ [M]^{21} & [M]^{22} & . & . & [M]^{2N} \\ . & . & . & . & . \\ . & . & . & . & . \\ [M]^{N1} & [M]^{N2} & . & . & [M]^{NN} \end{bmatrix} \quad \{dq\} = \begin{Bmatrix} \{du\}^1 \\ \{du\}^2 \\ . \\ . \\ \{du\}^N \end{Bmatrix}; \quad \{d\tilde{Q}\} = \{dp_i^J\} + \{R_i^J\}_k \qquad \text{(IV.77)}$$

where

$$dp_i^J = \left(p_i^J\right)_{k+1} - \left(p_i^J\right)_{k+1} \qquad \text{(IV.78)}$$

We remove all the known displacements from $\{dq\}$ and the corresponding terms from $\left[M\right]$ and $\{dQ\}$, then we get a new equation system:

$$\left[M_p\right]\{dq_p\} = \{dQ_p\} \qquad \text{(IV.79)}$$

where all the terms in $\{dQ_p\}$ are known.

From (IV.79) we can get $\{dq_p\}$ and, consequently, all the variables at the end of iteration *k+1*.

Iterations are performed until convergence is reached. The following convergence criterion is used.

For iteration *k*, let

$$REF_i = \frac{1}{N}\sum_{I=1}^{N}\left|\left({}^{B}\sigma_{ij}^{I}\right)_k A_j^{IJ}\right| \qquad i = 1,2$$

$$REF = REF_1 + REF_2$$

$$RES_i = \frac{1}{N}\sum_{I=1}^{N}\left|\left(R_i^I\right)_k\right| \qquad i = 1,2$$

$$RES = RES_1 + RES_2$$

$$RNORM = \frac{RES}{REF}$$

If *RNORM* is less than a user prescribed value, convergence is reached.

If the errors are small, *REF* is of the order of the average stress level (in absolute value) in the solid.

For some loading cases, this value can be zero or very close to zero. To avoid this problem, a user defined value *USER* is given and *REF* is calculated by

$$REF = max(REF_1 + REF_2, USER)$$

IV.8. Applications

IV.8.1. Plasticity and strain hardening in solids

In many materials, such as steel, aluminium and copper, plasticity and strain hardening are observed. An example of stress-strain curve for an elasto-plastic material with hardening is given at figure IV.2.

Unloading from a point B in the nonlinear zone, we find linear elastic behaviour with a modulus of elasticity equal to that experienced upon initial loading. Upon reloading, we find that the yield limit has increased. In rate-independent plasticity, the stress-strain law is independent of the rate of deformation but is dependent on the history of deformation.

Once the initial yield limit Y_0 has been passed, the total strain ε consists of an elastic strain ε_e and an inelastic strain ε_p and we have $\dot{\varepsilon} = \dot{\varepsilon}_e + \dot{\varepsilon}_p$ with $\varepsilon_e = \frac{\sigma}{E}$.

In visco-elasto-plastic materials, the stress-strain law also depends on the strain rate.

These notions are classical in Solid Mechanics and are not recalled here.

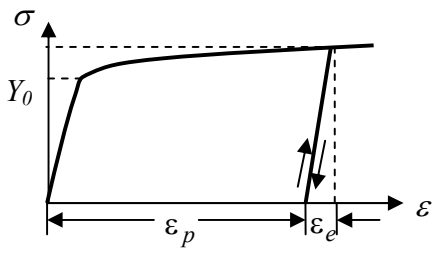

Figure IV.2. Stress-strain curve showing strain hardening

IV.8.2. Elasto-plastic material with von Mises linear hardening

As an example, we use the isotropic von Mises elasto-plastic model with linear hardening (figure IV.3) to calculate the matrix $\left[C_t^I\right]$.

Von Mises postulated a yield criterion which states that yielding occurs when the second invariant of the stress deviator tensor equals to a certain value which ideally depends only on the material itself.

The material parameters are:

E: Young's modulus.

ν : Poisson's ratio.

h_p : the plastic modulus.

R_e : the initial yield limit.

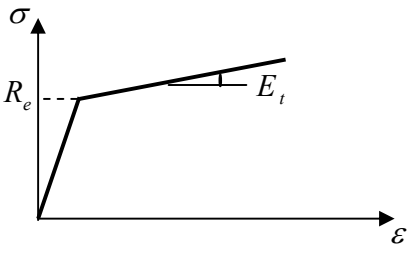

Figure IV.3. Uniaxial tensile stress-stain curve for an elasto-plastic material with von Mises linear hardening

For the integration of the stress-strain law during a time step, a classical method is the radial return [KRIEG R.D. and KRIEG R.D. (1977)].

We use the subscript *A* to denote the beginning of the time step and the subscript *B* for the end of the time step.

In the radial return method, the deviatoric part of stress is:

$$ {}^{B}\hat{\sigma}_{ij} = (1-\beta)\hat{\sigma}^{e}_{ij} \tag{IV.80} $$

where $\hat{\sigma}^{e}_{ij}$ is the elastic trial stress given by

$$ \hat{\sigma}^{e}_{ij} = {}^{A}\hat{\sigma}_{ij} + 2G\dot{\hat{\varepsilon}}_{ij}\Delta t \tag{IV.81} $$

in which $G = \dfrac{E}{2(1+\nu)}$ is the shear modulus.

The coefficient β is computed as follows:

$$ \beta = \frac{1-\dfrac{R_e}{\sqrt{3}J_2^e}}{1+\dfrac{h_p}{3G}} \tag{IV.82} $$

$$ J_2^e = \frac{\sqrt{\hat{\sigma}^{e}_{ij}\hat{\sigma}^{e}_{ij}}}{\sqrt{2}} \tag{IV.83} $$

$$ \frac{1}{h_p} = \frac{1}{E_t} - \frac{1}{E} \tag{IV.84} $$

where R_e is the initial yield limit, E_t the tangent modulus and h_p is the plastic modulus.

After some developments, we get an equation of the form:

$$ \{d\hat{\sigma}\} = 2G[\eta]\{d\hat{\sigma}^{e}\} = 2G[\eta]\{d\dot{\hat{\varepsilon}}\}\Delta t \tag{IV.85} $$

where

$$ [\eta] = (1-\beta)\begin{bmatrix} 1 & 0 & 0 \\ 0 & 1 & 0 \\ 0 & 0 & 1 \end{bmatrix} - \frac{R_e}{2\sqrt{3}(J_2^e)^3(1+\dfrac{h_p}{3G})}\begin{bmatrix} \hat{\sigma}^{e}_{11}\hat{\sigma}^{e}_{11} & \hat{\sigma}^{e}_{11}\hat{\sigma}^{e}_{22} & 2\hat{\sigma}^{e}_{11}\hat{\sigma}^{e}_{12} \\ \hat{\sigma}^{e}_{22}\hat{\sigma}^{e}_{11} & \hat{\sigma}^{e}_{22}\hat{\sigma}^{e}_{22} & 2\hat{\sigma}^{e}_{22}\hat{\sigma}^{e}_{12} \\ \hat{\sigma}^{e}_{12}\hat{\sigma}^{e}_{11} & \hat{\sigma}^{e}_{12}\hat{\sigma}^{e}_{22} & \hat{\sigma}^{e}_{12}\hat{\sigma}^{e}_{12} \end{bmatrix} \tag{IV.86} $$

The volumetric part of stress is:

$$ {}^{B}\sigma_m = {}^{A}\sigma_m + 3\chi\dot{\varepsilon}_m\Delta t \tag{IV.87} $$

in which $\chi = \dfrac{E}{3(1-2\nu)}$ is the bulk modulus and $\sigma_m = \dfrac{1}{3}\sigma_{ii} = \dfrac{1}{3}(\sigma_{11}+\sigma_{22}+\sigma_{33})$ is the mean stress.

From (IV.87), we get:

$$d\sigma_m = 3\chi\, d\dot{\varepsilon}_m \Delta t \tag{IV.88}$$

Consequently

$$\{d\sigma\} = \{d\hat{\sigma}\} + d\sigma_m \{\delta\} \quad \text{with} \quad \{\delta\} = \begin{Bmatrix} 1 \\ 1 \\ 0 \end{Bmatrix}$$

Introducing (IV.85) and (IV.88) , we obtain:

$$\{d\sigma\} = \left[C_t^I\right]\{d\dot{\varepsilon}\}\Delta t \tag{IV.89}$$

in which,

$$\left[C_t^I\right] = 2G[\eta] + \frac{1}{3}(3\chi[I] - 2G[\eta])\{\delta\}\{\delta\}^T \tag{IV.90}$$

with $[I]$ the unit matrix.

IV.8.3. Patch tests

A set of patch tests in simple tension and in pure shear are performed to validate the method.

All the information and results are collected in figures IV.4 to IV.7.

For the case of figure IV.4, the stresses are within machine precision, no matter the value of the convergence criterion. Only one iteration is required to reach convergence since hardening is linear and the loading is a linear function of time.

For the cases of figure IV.5 and IV.6, the loading is a combination of sine functions.

For the calculation of *RNORM*, the value of *USER = 20*, that is equal to the maximum stress level imposed during the loading.

The chosen convergence value is $RNORM \leq 10^{-8}$.

The following variable is defined to evaluate the computation error:

$$L2\,norm(\sigma) = \frac{\sum_{K=1}^{N} A_K \sqrt{(\sigma_{ij}^K - \sigma_{ij}^{exact})(\sigma_{ij}^K - \sigma_{ij}^{exact})} \Big/ \sum_{K=1}^{N} A_K}{\sum_{K=1}^{N} A_K \sqrt{\sigma_{ij}^{exact}\sigma_{ij}^{exact}} \Big/ \sum_{K=1}^{N} A_K}$$

Figure IV.7 shows the evolution of $L2norm(\sigma)$ with time.

Because the loading is not a linear function of time, we have more than one iteration in the plastic domain to reach convergence.

From this figure we can see that, at some time steps, $L2norm(\sigma)$ is not as small as for others. This is due to the fact that we define:

$RNORM = \dfrac{RES}{REF}$ and $REF = max(REF_1 + REF_2, USER)$.

Hence, according to the convergence criterion, we have $\dfrac{RES}{REF} \le 10^{-8}$, from which we can get $RES \le 10^{-8} * REF \le 10^{-8} * 20 = 2 * 10^{-7}$

This explains the observed result.

Loading and boundary conditions	Stress-strain curve
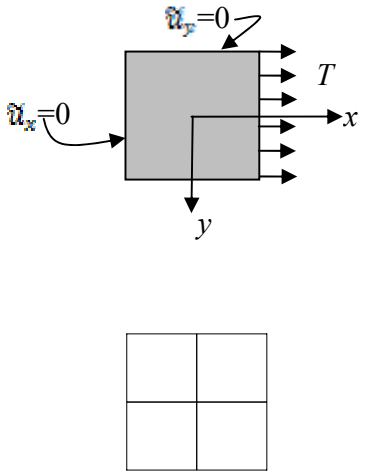	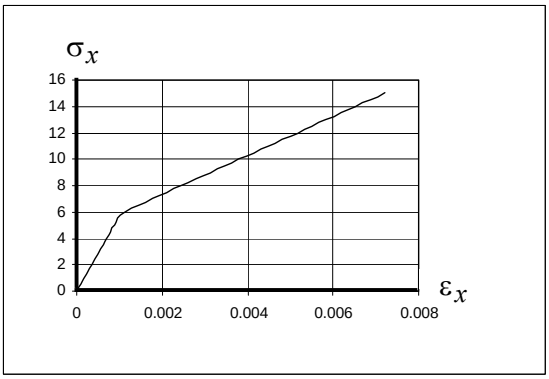
Case 1 (4 nodes): a square domain submitted to simple tension. The applied surface traction is given by $T = t$ t varies from 0 to 2 seconds by time steps $\Delta t = 0.05s$ each.	

Figure IV.4. Patch test, case 1

Loading and boundary conditions	Stress-strain curve
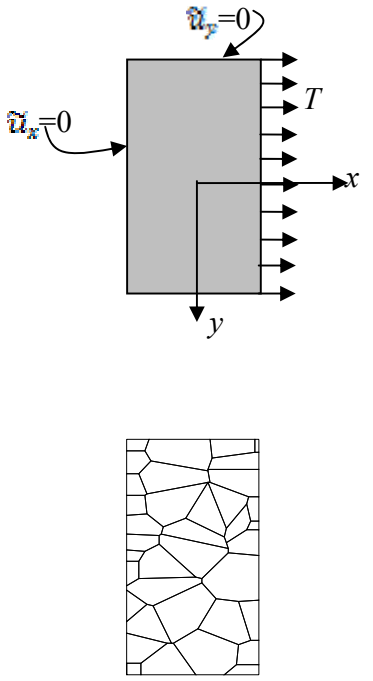	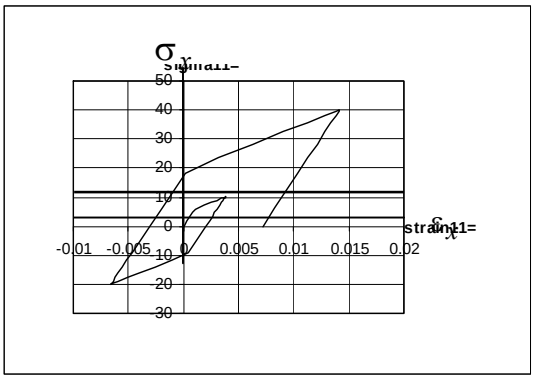

Case 2 (38 nodes): a rectangular domain submitted to simple tension.
The applied surface traction is given by:

$T = 5\,sin(\pi * t)$ when $0 \le t \le 1$

$T = 10\,sin(\pi * t)$ when $1 \le t \le 2$

$T = 20\,sin(\pi * t)$ when $2 \le t \le 3$

t varies from 0 to 3 seconds by time steps $\Delta t = 0.05s$

Figure IV.5. Patch test, case 2

Loading and boundary conditions	Stress-strain curve
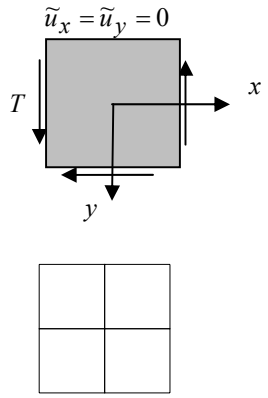	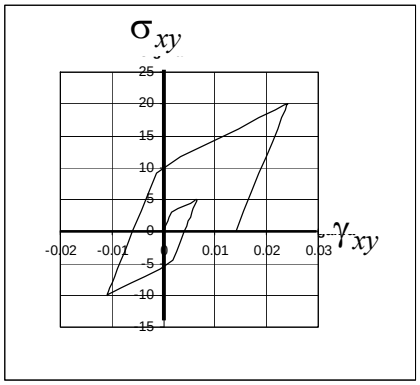

Case 3 (4 nodes): a square domain submitted to pure shear.
The applied surface traction is given by:

$T = 5\,sin(\pi * t)$ when $0 \le t \le 1$

$T = 10\,sin(\pi * t)$ when $1 \le t \le 2$

$T = 20\,sin(\pi * t)$ when $2 \le t \le 3$

t varies from 0 to 3 seconds by time steps $\Delta t = 0.05s$

Figure IV.6. Patch test, case 3

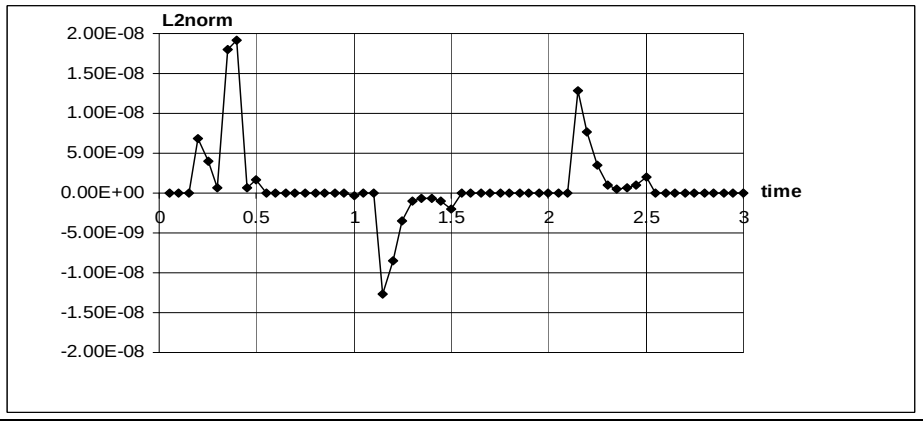

Figure IV.7. Patch test, case 3: evolution of $L2\,norm(\sigma)$

IV.8.4. Pure bending

The material is that of figure IV.3.

The material parameters are:

$E = 200000$ MPa; $\nu = 0.3$; $E_t = 1488.83$ MPa; $R_e = 300$ Mpa; $G = 76923$ MPa; $h_p = 1500$ MPa

The loading and boundary conditions are shown on figure IV.8.

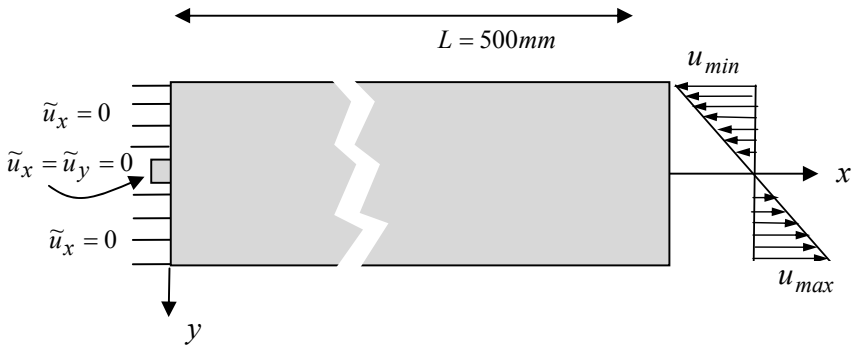

Figure IV.8. Geometry and loading for the elasto-plastic bending

They are similar to the elastic case but the loading is obtained by imposing displacements to the right end of the beam as indicated on figure IV.8.

We define the u_{min} and the u_{max} as functions of time:

$u_{min} = u_{max} = 0.02 * 3\sqrt{3} * t$ if $0 \le t \le 1$

$u_{min} = u_{max} = 0.01 * 3\sqrt{3} * (4 - 2 * t)$ if $1 \le t \le 2$

The time step is: $\Delta t = 0.05s$.

The curvature of the deformed beam is a function of time and is given by:

$$\chi(t) = \frac{u_{\max}(t)}{h * L}$$

and we have:

$\varepsilon(t) = \chi(t) * y$

$\sigma = E\varepsilon$ if $\varepsilon < \varepsilon_e = \frac{R_e}{E}$

$\sigma = R_e + E_t(\varepsilon - \varepsilon_e) \quad \text{if} \quad \varepsilon > \varepsilon_e$

The bending moment of the deformed beam is related to its curvature by:

$$M_{theory} = 2\left\{\left[\frac{1}{3}\frac{{R_e}^3}{(E\,\chi)^2}\right] + \frac{1}{2}(R_e - E_t\varepsilon_e)\left[h^2 - \left(\frac{R_e}{E\,\chi}\right)^2\right] + \frac{1}{3}E_t\chi\left[h^3 - \left(\frac{R_e}{E\,\chi}\right)^3\right]\right\}$$

On the other hand, from the numerical calculation, we get

$$M_{num} = \int_{-h}^{h} ry dA = \frac{2r{h}^2}{3}$$

where r is the support reaction of the edges where the displacements are imposed.

We can get the numerical value of the strain energy by:

$$W_{I\_num} = \sum_I A_I \int_0^t \left\langle \sigma^I \right\rangle \{\dot{\varepsilon}\}^I dt$$

Results of different calculations are given in table IV.4 and summarized in figure IV.9.

Another numerical solution for the plane strain case has been calculated by the method proposed in [ROSSI B. et al, (2007)]. It is based on the direct integration of the differential equations for the pure bending case in plane strain. We denote the energy obtained from this method as W_0, and the moment as M_0.

The error on the strain energy is calculated by: $Error = \dfrac{W_{I\_num} - W_0}{W_0}$

The values of the strain energy at time $t = 2s$ for different numbers of nodes *N* are given in table IV.4.

Figure IV.9 shows the moment-curvature curves of the method proposed in this chapter and in [Rossi B. et al (2007)] by direct integration of the differential equations of Solid Mechanics..

Table IV.4. Convergence on energy.
$W_0 = 4265.11J$ at time $t = 2s$

N *(random=0.1)*	W_{I_num} *(J)*
76	4531.33
140	4342.65
244	4290.00

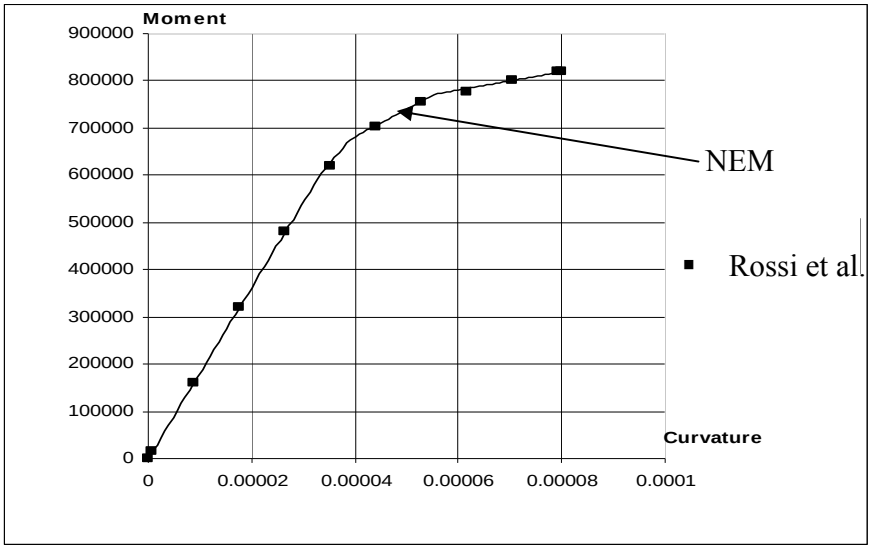

Figure IV.9. Comparison of the moment-curvature curves

The L2 norm of the error on the displacements is defined by:

$$L2norm(u) = \frac{\sum_{i=1}^{N} \sqrt{(u_i^{theory} - u_i^{num}) * (u_i^{theory} - u_i^{num})}}{L\,N}$$

where u_i^{theory} are the nodal displacements computed from the analytical solution while u_i^{num} are the nodal displacements obtained by the present numerical method. N is the number of nodes.

Figure IV.10 shows the convergence of the displacements at time $t = 2s$.

In addition, a case of cyclic loading is also performed with:

$|u_{min}| = u_{max} = sin(t\pi) \quad 0 \le t < 1 \ s$

$|u_{min}| = u_{max} = 2\,sin(t\pi) \quad 1 \le t < 2 \ s$

$|u_{min}| = u_{max} = 4\,sin(t\pi) \quad 2 \le t < 4 \ s$

t varies from 0 to 3 seconds and $\Delta t = 0.01s$.

Figure IV.11 shows the moment - curvature curve.

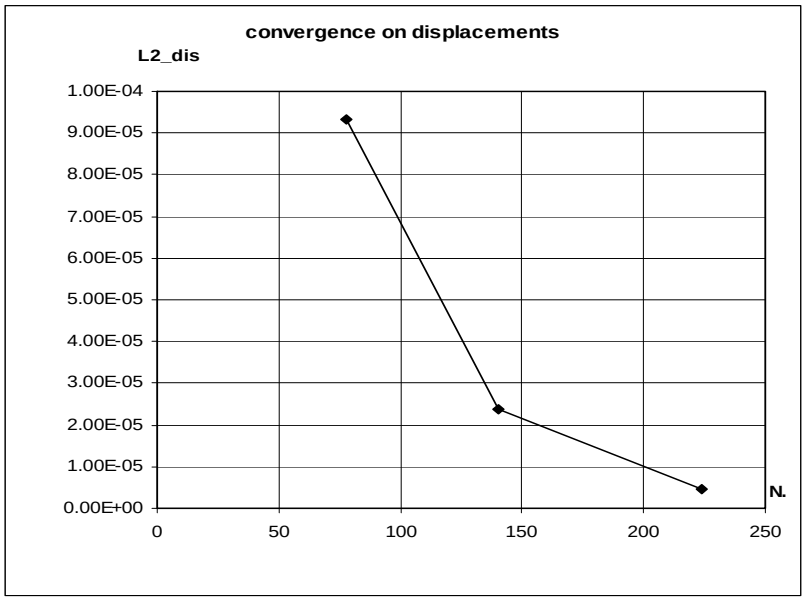

Figure IV.10. Convergence of $L2norm(u)$

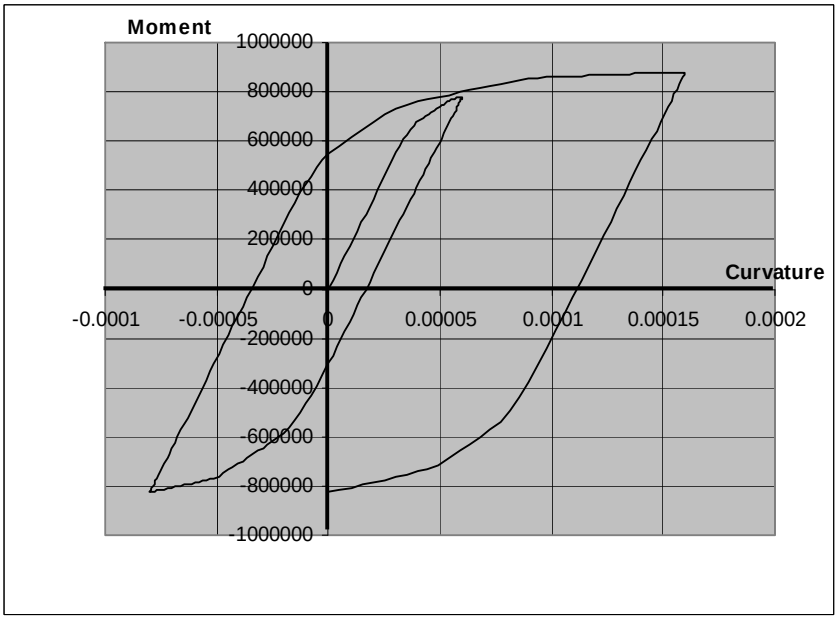

Figure IV.11. Moment-curvature curve for cyclic loading.

IV.8.5. Square membrane with a circular hole

The last application in the elasto-plastic domain is the square membrane with a circular hole, the geometry of which is defined in figure III.10 (chapter III).

The material is elasto-plastic with von Mises linear hardening.

The material parameters are:

$E = 200000$ MPa; $\nu = 0.3$; $E_t = 9523.81$ MPa; $R_e = 300$ Mpa; $G = 76923$ MPa; $h_p = 10000$ MPa

The loading $0 \le T \le 350 MPa$ is a linear function of time.

Unit thickness and plane strain conditions are assumed.

The results for the strain energy convergence are summarized in table IV.5.

For the present method, 2 integration points per Voronoi edge are used. For the finite element method, classical 4 nodes isoparammetric elements have been used with 4 Gauss integration points for the numerical integrations on the area of the elements.

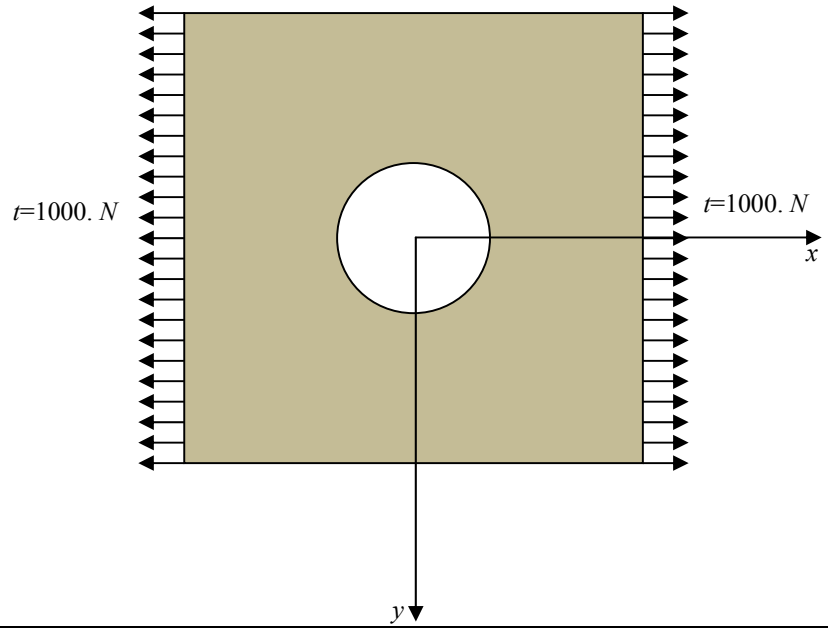

Figure III.10.a. Geometry and loading for the square membrane with a circular hole

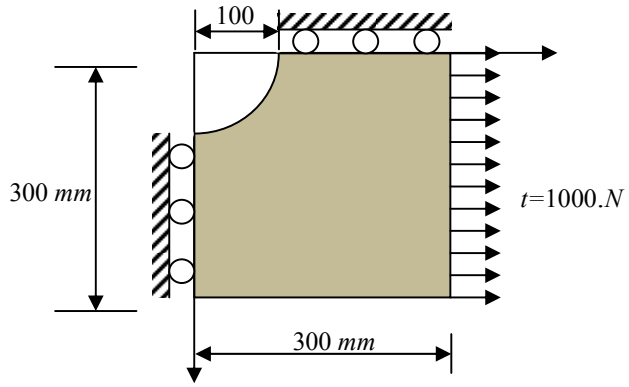

Figure III.10.b. Square membrane with a circular hole: studied model

Table IV.5. Strain energy (*J*) for the square membrane with a circular hole Elasto-plastic case					
Present method			Finite elements		
N	*t*=1*s*	*t*=3.5*s*	*N*	*t*=1*s*	*t*=3.5s
36	2855	302707	33	2689	196815
121	2837	297164	119	2770	247143
441	2819	294086	445	2803	268669
1681	2811	295292	5251	2811	278514

At *t*=1*s*, the membrane is still in the elastic domain while it is well in the elasto-plastic range at *t*=3.5*s*.

The strain energy convergence curves at *t*=1*s* and *t*=3.5*s* are presented in figure IV.12.

It is clearly seen that the present approach converges from above while, as it is well known, the FEM converges from below in the present case.

It is also observed that, for the same number of nodes, the present results are closer to convergence than the FEM results.

The displacements of the right side of the membrane, i.e. of the line *x*=300 *mm*, are given in figures IV.13 and IV.14 at *t*=1*s* and *t*=3.5*s* respectively.

From figures IV.13 and 14, it is observed that, when the membrane remains in the elastic domain (*t=1s*), the FEM and the NEM results practically coincide for a sufficient number of nodes. However, in the plastic range (*t=3.5 s*), there remains a slight difference even with the large numbers of nodes.

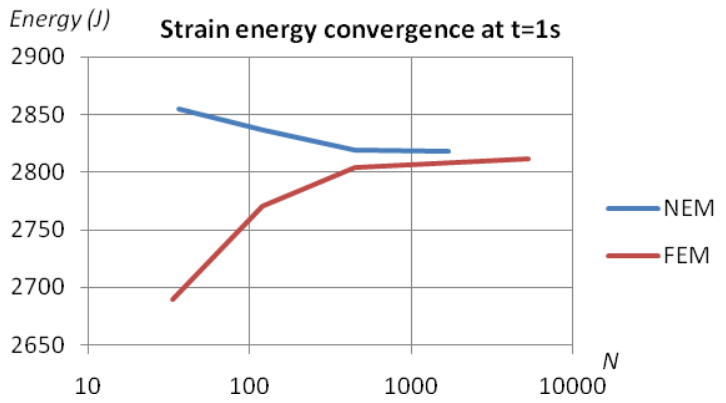

Figure IV.12 a. Strain energy convergence: comparison of the present approach with FEM at time = 1s

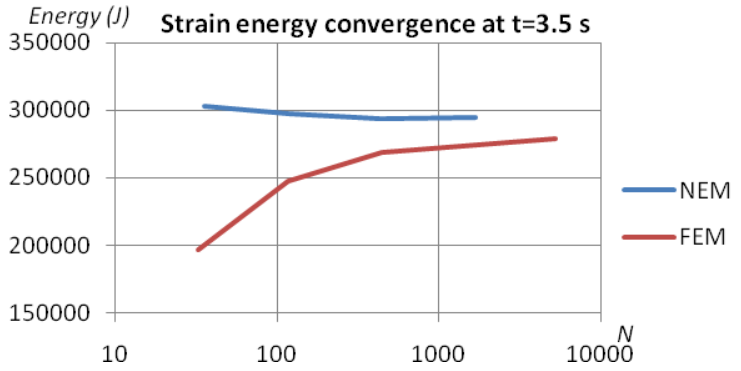

Figure IV.12 b. Strain energy convergence: comparison of the present approach with FEM at time = 3.5 s

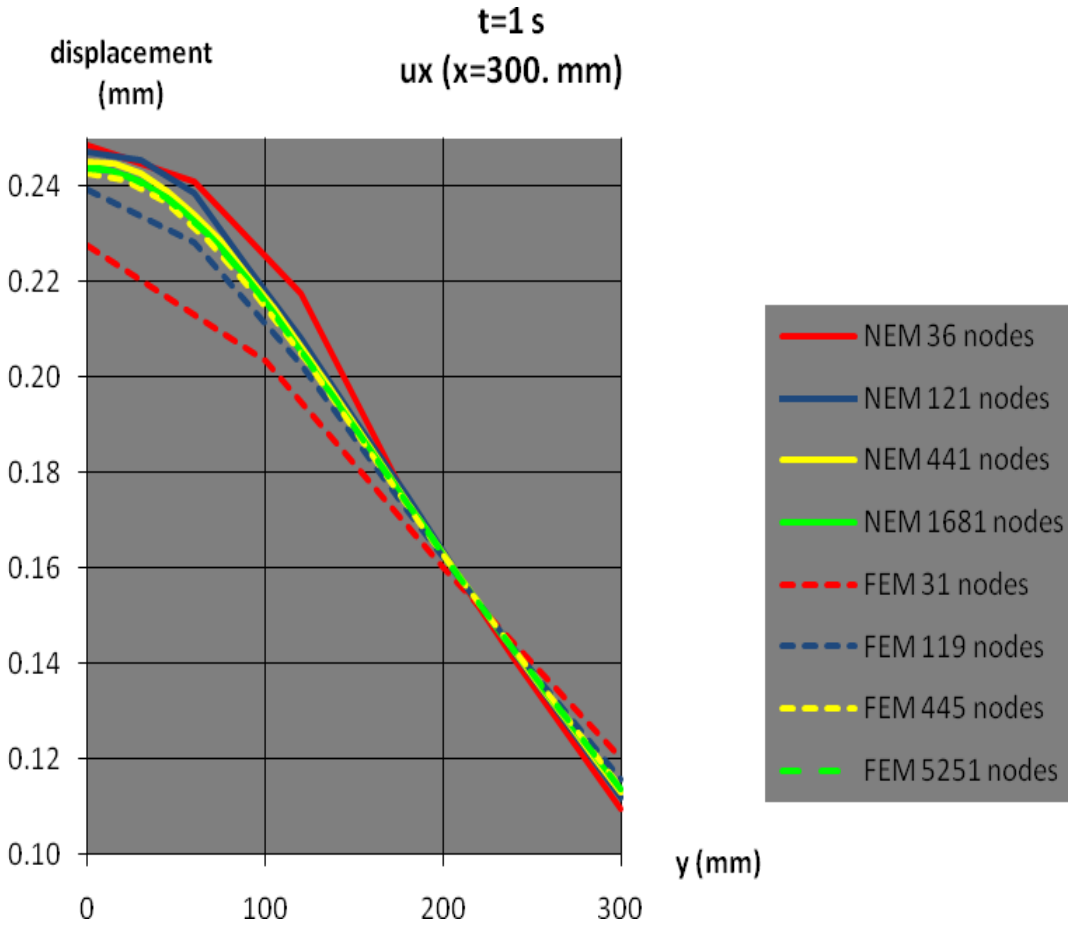

Figure IV.13. Displacements u_x on the boundary x=300mm at time t=1 s

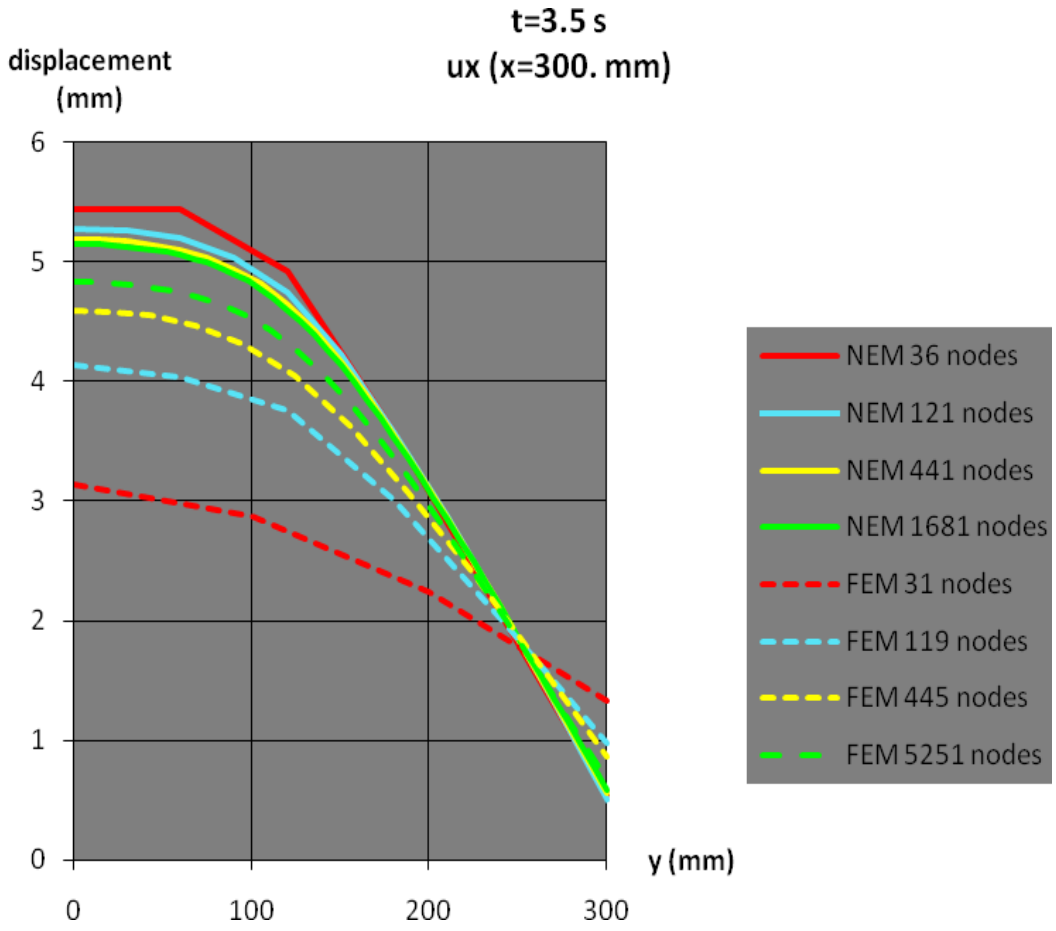

Figure IV.14. Displacements u_x on the boundary x=300mm at time t=3.5 s

IV.9. Conclusion

The Fraeijs de Veubeke variational principle has been used to develop a natural neighbours method in which the displacements, stresses, strains and surface support reactions can be discretized separately.

This approach, which has been developed for linear elastic problems in chapter III is extended to the geometrically linear and materially non linear case in this chapter.

With the present approach, the properties of linear elastic case remain valid in non linear case. That is, in the absence of body forces, the calculation of integrals over the area of the domain is avoided: only integrations on the edges of the Voronoi cells are required,

for which classical Gauss numerical integration with 2 integration points is sufficient to pass the patch test.

In addition, the derivatives of the nodal shape functions are not required in the resulting formulation.

This approach presents a clear advantage over more classical methods using integrations over the area of the domain with the help of a sometimes very high number of integration points.

Exactly as in linear elastic problems, the same 2 ways can be used to impose displacements here..

- In the spirit of the FdV variational principle, boundary conditions of the type $u_i = \widetilde{u}_i$ on S_u can be imposed in the average sense; hence, any function $\widetilde{u}_i = \widetilde{u}_i(s)$ can be accommodated by the method;
- However, since the natural neighbours method is used, the interpolation of displacements on the solid boundary is linear between 2 adjacent nodes. So, if the imposed displacements $\widetilde{u}_i$ are linear between 2 adjacent nodes, they can be imposed exactly. This is obviously the case with $\widetilde{u}_i = 0$. In such a case, it is equivalent to impose the displacements of these 2 adjacent nodes to zero.

The applications to an elasto-plastic model with von Mises linear hardening have shown that elasto-plastic patch tests in pure tension and in pure shear are successfully passed.

Calculations for the elasto-plastic bending case show a good convergence to the solution based on the direct integration of the equations [ROSSI.B et al (2007)].

The example of the square membrane with circular hole has shown that the present approach compares favourably with the classical FEM.

Although the presented applications have been developed for a von Mises linear hardening elasto-plastic model, the theory obviously applies also for all kinds of non linear material models.